



# Dispersion relation of flexural waves in metamaterial plates with periodic shunted piezo-patches

Edson J. P. de Miranda Jr.<sup>1,2,3,a</sup>, José M. C. Dos Santos<sup>3,b</sup>

<sup>1</sup>Federal Institute of Maranhão, IFMA-EIB-DE  
Rua Afonso Pena, 174, CEP 65010-030, São Luís, MA, Brazil

<sup>2</sup>Federal Institute of Maranhão, IFMA-PPGEM  
Avenida Getúlio Vargas, 4, CEP 65030-005, São Luís, MA, Brazil

<sup>3</sup>University of Campinas, UNICAMP-FEM-DMC  
Rua Mendelejev, 200, CEP 13083-970, Campinas, SP, Brazil

<sup>a</sup>edson.jansen@ifma.edu.br, <sup>b</sup>zema@unicamp.br

**Abstract.** The wave propagation in a 2-D mechanical metamaterial plate with periodic arrays of shunted piezo-patches is investigated. This piezoelectric mechanical metamaterial plate is capable of filtering the propagation of flexural waves over a specified range of frequency, called band gaps. The dispersion relations are obtained by the improved plane wave expansion (IPWE) and extended plane wave expansion (EPWE) methods. The Bragg-type and locally resonant band gaps are opened up. The shunt circuits influence significantly the propagating and the evanescent modes. The results can be used for elastic wave attenuation using 2-D piezoelectric periodic structures.

**Keywords:** Periodicity, Band gaps, Shunt circuits, Evanescent waves

## 1 Introduction

Recently, the piezoelectric shunt damping combined with the concept of periodic structures created the piezoelectric metamaterials (PMs). In terms of wave attenuation, the advantage of using PMs is the formation of both Bragg-type and locally resonant band gaps [1]. These forbidden bands are regions of frequency where there are only evanescent waves [2, 3]. In addition, the 1-D [4] and 2-D [1, 5, 6] PMs have been extensively studied by experimental techniques and numerically.

Chen (2018) [1] obtained the dispersion curves of 2-D acoustic metamaterials with shunting circuits by using the finite element (FE) method with COMSOL. He observed an attenuation zone around the band gap location, in which the wave propagation is decayed strongly.

Xiao *et al.* (2020) [6] designed an adaptive hybrid laminate acoustic metamaterial composed of carbon-fiber-reinforced polymer and a periodic array of piezoelectric shunting patches attached to the laminate. They demonstrated by using FE approach that the lightweight adaptive hybrid laminate metamaterial with the shunting circuits can remarkably suppress wave propagation compared to the un-shunted case. Moreover, they discussed the effects of the laminate's parameters as well as the shunting circuits on the band gap's location and bandwidth. They also introduced a negative capacitance shunting circuit into the piezoelectric patches, in order to enlarge the bandwidth.

In this investigation, the dispersion relations are numerically obtained by the improved plane wave expansion (IPWE) [2, 3, 7] and extended plane wave expansion (EPWE) [2, 3, 8] methods. First, the cases of open and short circuits are studied. Next, two types of closed electrical circuits are considered, *i.e.*, resistive and resonant circuits.

## 2 Simulated Examples

The IPWE,  $\omega(\mathbf{k})$ , and the EPWE,  $\mathbf{k}(\omega)$ , are used to compute the propagating and evanescent modes of the dispersion relation, respectively, where  $\mathbf{k}$  is the wave number and  $\omega$  is the angular frequency. The formulations are

not derived for brevity. The Kirchhoff-Love [9, 10] thin plate theory is used to model the 2-D PMs with periodic arrays of shunted piezo-patches with a square cross section area.

Figure 1 sketches the top (a) and front (b) views of the 2-D PM unit cell. The piezoelectric patches with shunting circuits connected in parallel, for the cases of resistive ( $Z^{SU} = R$ ) and resonant ( $Z^{SU} = R + i\omega L$ ) circuits, are illustrated in (b), where  $Z^{SU}$  is the electrical impedance of the shunting circuit,  $i = \sqrt{-1}$ ,  $R$  is the resistance and  $L$  is the inductance of the electrical circuit. In Fig. 1 (c), it is shown the first irreducible Brillouin zone (FIBZ) [11] of the 2-D PM for a square lattice, where the FIBZ points are  $\Gamma$  (0, 0), X ( $\pi/a$ , 0) and M ( $\pi/a$ ,  $\pi/a$ ) and  $a$  is the lattice parameter.

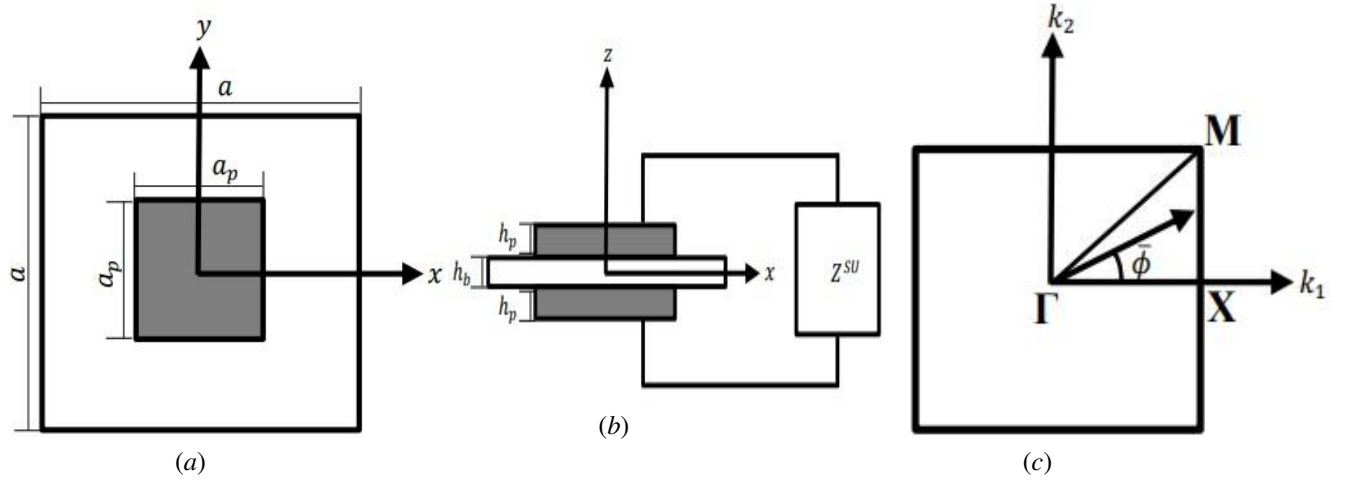


Figure 1. Top (a) and front (b) views of the 2-D piezoelectric metamaterial thin plate unit cell. Piezoelectric patches with shunting circuits connected in parallel (b), for the cases of resistive ( $Z^{SU} = R$ ) and resonant ( $Z^{SU} = R + i\omega L$ ) circuits. First irreducible Brillouin zone of the 2-D piezoelectric metamaterial for a square lattice.

The physical parameters [6] of the plate (b) and the piezoelectric patches (p) are listed in Table 1. It should

Table 1. Geometry and material properties of the plate (b) and piezoelectric patch (PZT-5H) (p).

Geometry/Property	Value
Lattice parameter ( $a$ )	0.06 m
Piezoelectric patch length ( $a_p$ )	0.03 m
Plate thickness ( $h_b$ )	0.0016 m
Piezoelectric patch thickness ( $h_p$ )	0.0002 m
Mass density ( $\rho_b, \rho_p$ )	$1.6 \times 10^3$ kg/m <sup>3</sup> , $7.5 \times 10^3$ kg/m <sup>3</sup>
Young's modulus ( $E_b, E_p$ )	$181 \times 10^9$ N/m <sup>2</sup> , $60.606 \times 10^9$ N/m <sup>2</sup>
Poisson's ratio ( $\nu_b, \nu_p$ )	0.28, 0.2897
Compliance coefficient at constant electric field ( $s_{11}^E$ )	$16.5 \times 10^{-12}$ 1/Pa
Compliance coefficient at constant electric field ( $s_{12}^E$ )	$-4.78 \times 10^{-12}$ 1/Pa
Piezoelectric strain constant ( $d_{31}$ )	$-2.74 \times 10^{-10}$ C/N
Dielectric constant ( $\epsilon_{33}^\sigma$ )	$3400\epsilon_0$
Electromechanical coupling coefficient ( $k_{31}$ )	0.35
Electrical capacitance of the piezo at constant strain ( $C_p^\epsilon$ )	$118.87 \times 10^{-9}$ F

be pointed out that the plate and piezoelectric patch loss factors are not considered.

Figure 2 shows the complex dispersion relation of the 2-D PM plate for the case of open circuit ( $Z^{SU} \rightarrow \infty$ ) regarding 49 plane waves and  $\Gamma X$  direction,  $\bar{\phi} = 0$ , (from now on).

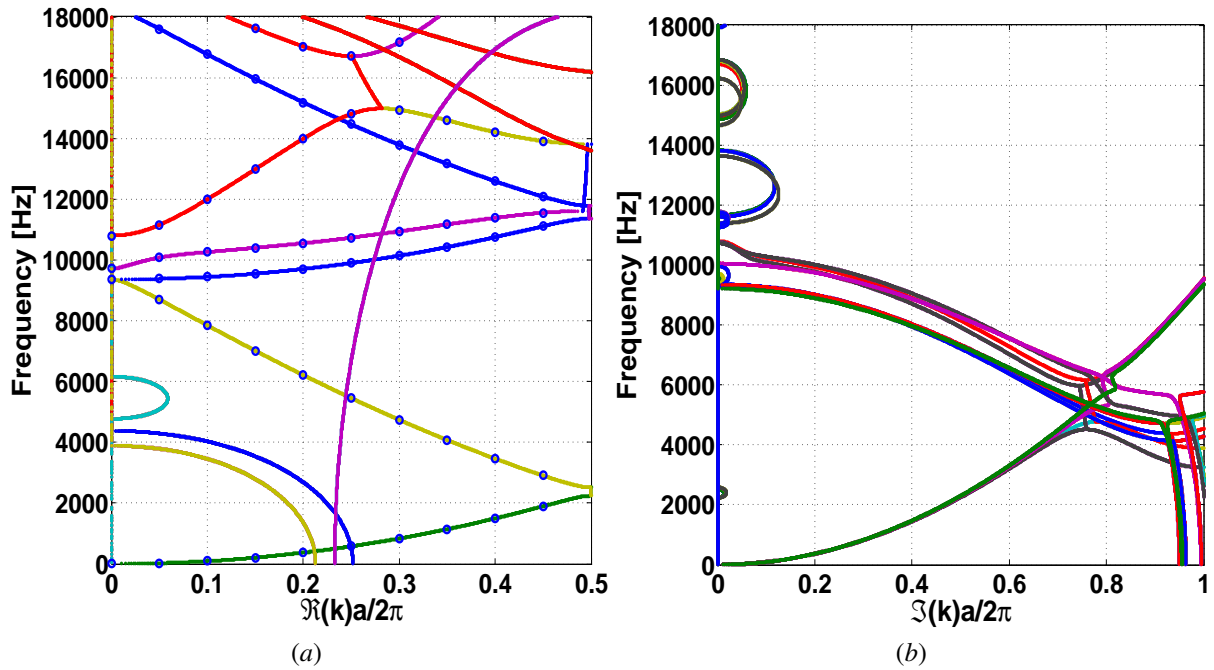


Figure 2. Complex dispersion relation of the 2-D PM plate with open circuit ( $Z^{SU} \rightarrow \infty$ ) computed by (a) IPWE (blue circles) and (a – b) EPWE (points) methods.

In Figure 2 (a), one can note that IPWE (blue circles) can identify only the propagating modes. The evanescent modes with complex wave numbers are obtained by the EPWE (points). For EPWE calculation, a  $\Delta f = 1$  Hz is regarded. The band gaps in Figure 2 are created only by Bragg scattering, since there is no electrical resonance. The Bragg-type band gaps can be directly observed between the propagating modes obtained by IPWE.

Figures 3 and 4 show the complex dispersion relations for the cases of short ( $Z^{SU} = 0$ ) and resistive ( $R = 50 \Omega$ ) circuits. The behaviours are similar, however, the resistor slightly increases the total piezoelectric loss factor (Fig. 4). It should be underlined that the IPWE cannot be directly used to compute the dispersion relations for the cases of closed circuit (resistive and resonant circuits), since there are some properties depending on the frequency (see [6] for these expressions).

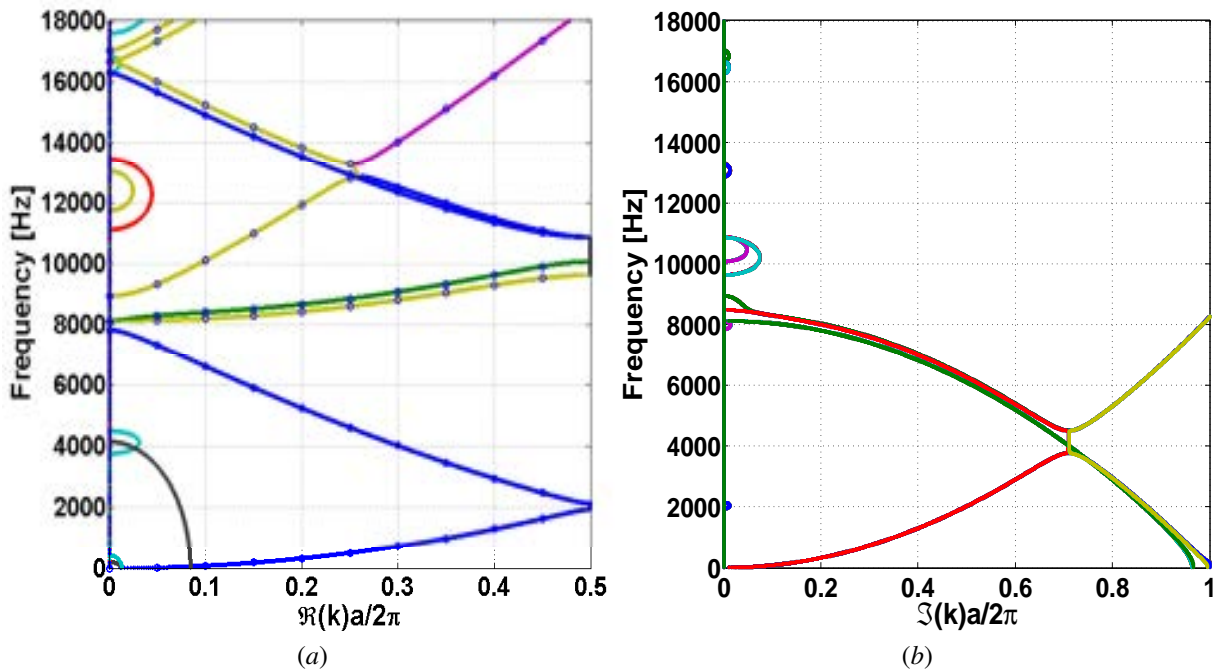


Figure 3. Complex dispersion relation of the 2-D PM plate with short circuit ( $Z^{SU} = 0$ ) computed by (a) IPWE (blue circles) and (a – b) EPWE (points) methods.

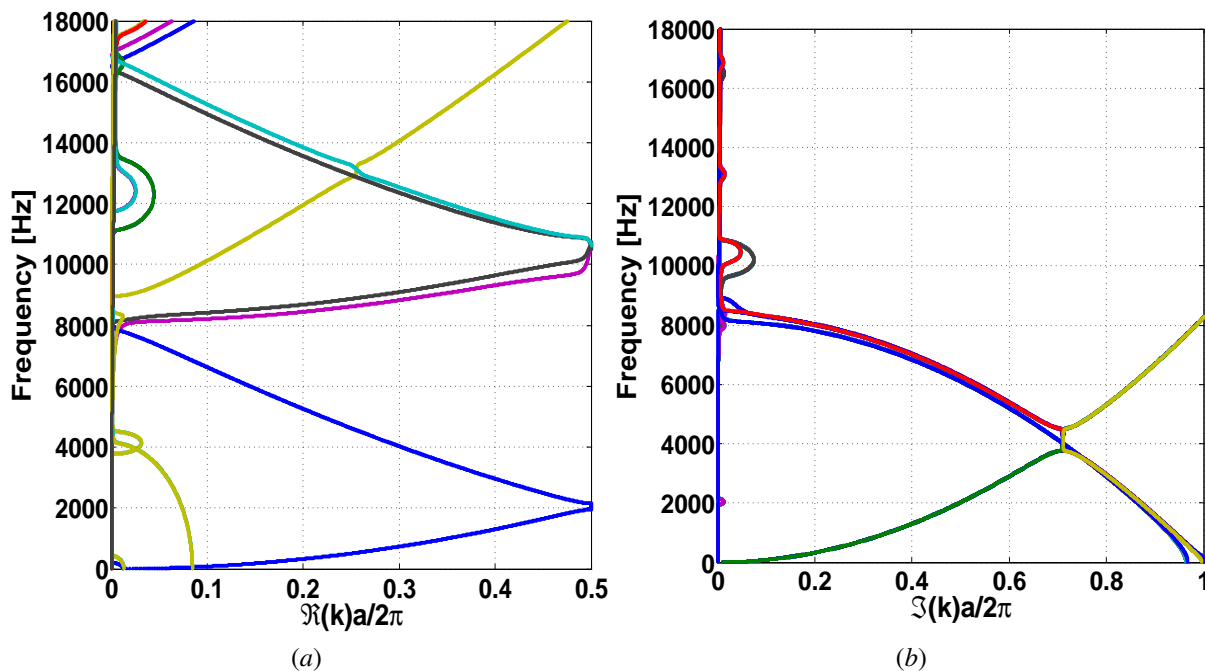


Figure 4. Complex dispersion relation of the 2-D PM plate with resistive circuit ( $R = 50 \Omega$ ) computed by EPWE.

Figure 5 illustrates the complex dispersion relation for the case of resonant circuit ( $f_T = 768.786$  Hz), where  $f_T$  is the resonance of the electrical circuit. The locally resonant band gap can be observed in Fig. 5 around the resonant frequency. The resonance is easily identified considering for instance the first four modes (see Fig. 6).

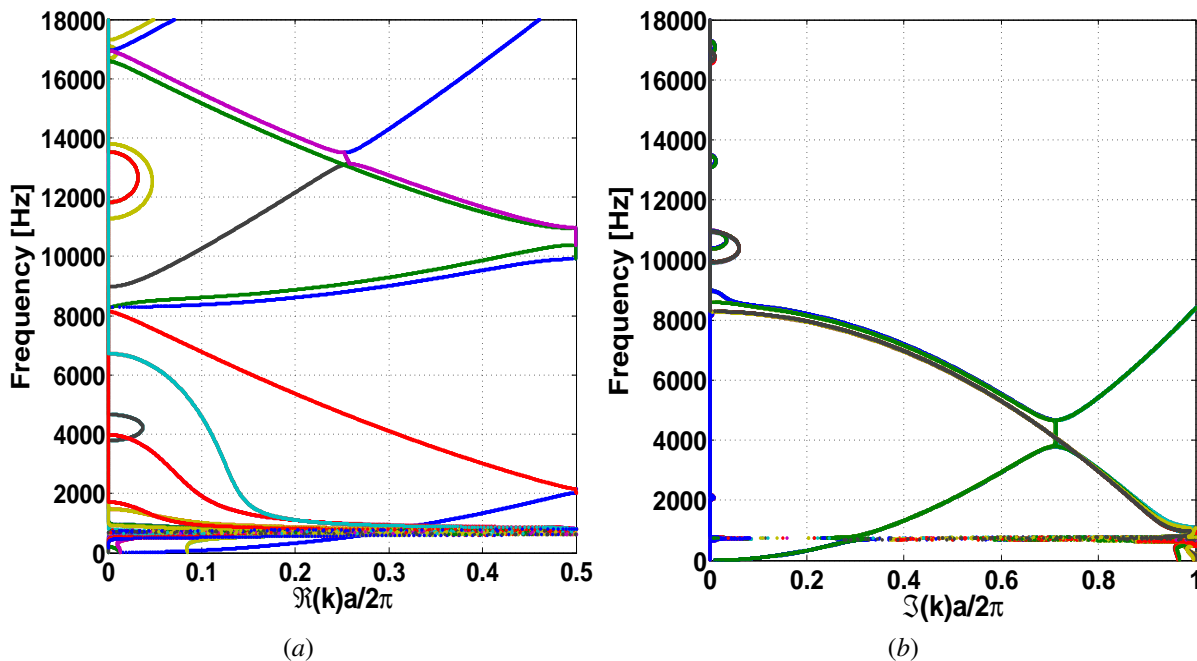


Figure 5. Complex dispersion relation of the 2-D PM plate with resonant circuit ( $f_T = 768.786$  Hz) computed by EPWE.

In Fig. 7, it is presented the complex dispersion relation zoom around the locally resonant band gap regarding only the second mode. It should be pointed out that Fig. 7 (b) does not consider all the most accurate imaginary components (those associated with the real components which lie inside and around the first Brillouin zone [2]). Moreover, the unit cell wave attenuation ( $\Im\{\mathbf{k}\}a$ ) shown in Fig. 7 (b) is comparable to those one obtained by the mechanical metamaterials with periodic resonators [2, 3].

Figure 8 compares the complex dispersion relation zoom around the locally resonant band gap considering only the second mode obtained by the EPWE (blue points) and conventional EPWE (green points) approaches,

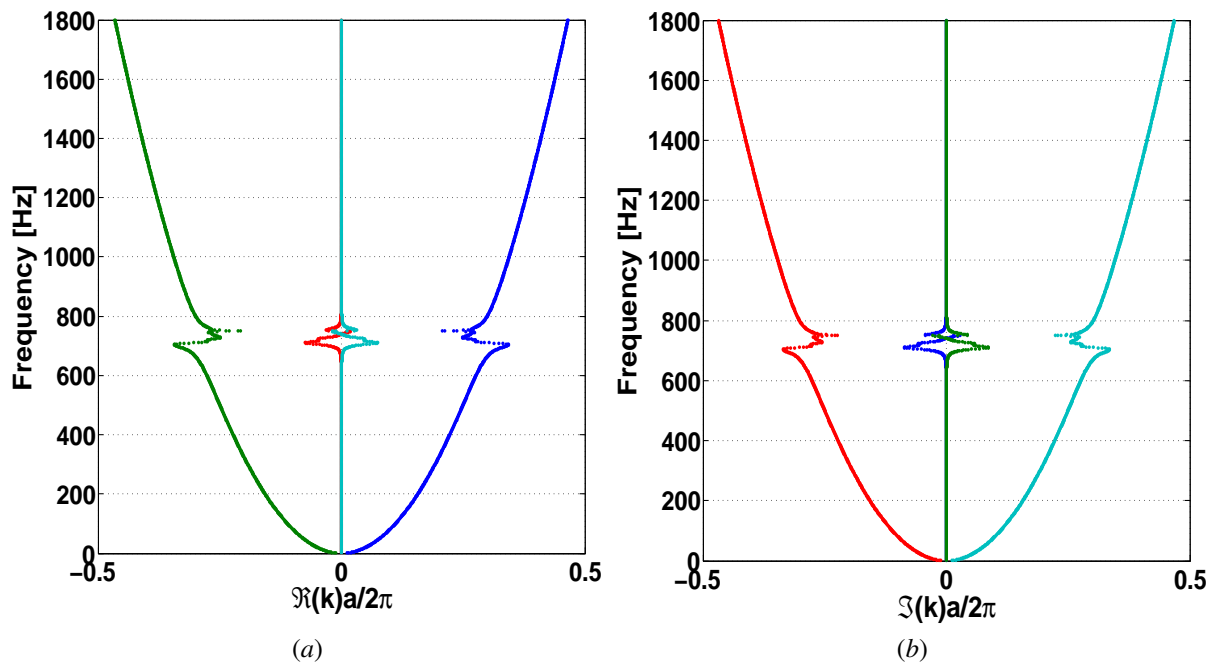


Figure 6. Complex dispersion relation zoom (only the first four modes) around the locally resonant band gap of the 2-D PM plate with a resonant circuit ( $f_T = 768.786$  Hz) computed by EPWE.

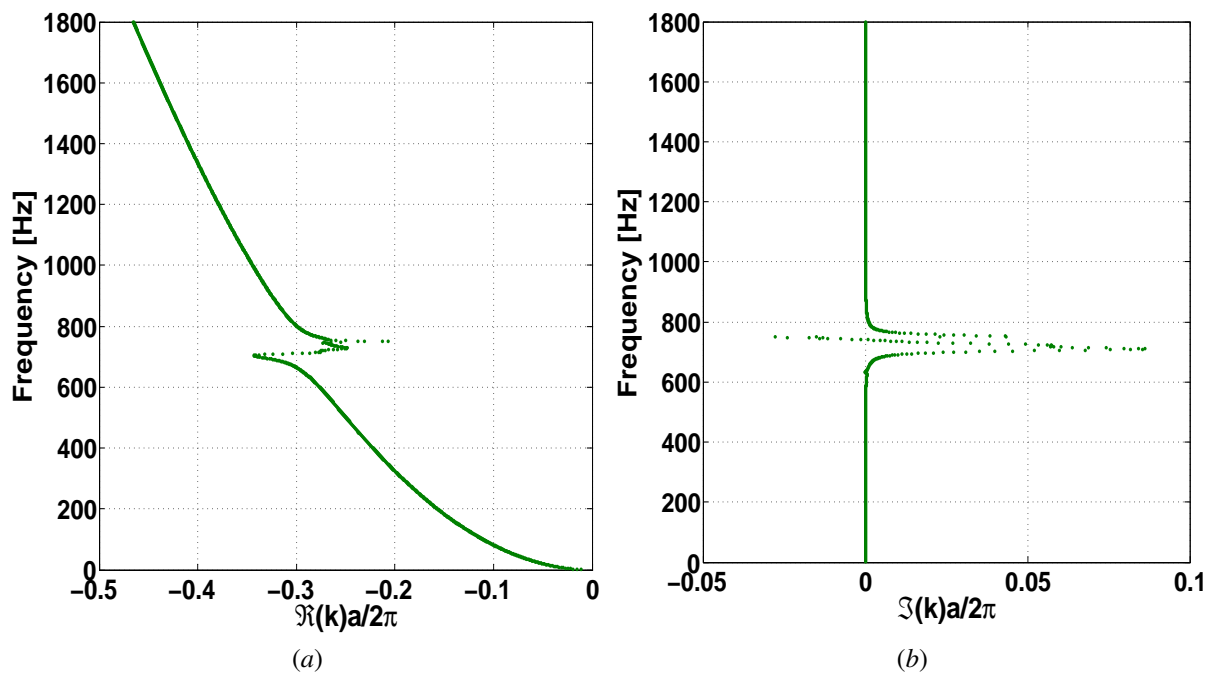


Figure 7. Complex dispersion relation zoom (only the second mode) around the locally resonant band gap of the 2-D PM plate with a resonant circuit ( $f_T = 768.786$  Hz) computed by EPWE.

with  $\Delta f = 0.1$  Hz. It should be highlighted that the EPWE used until now is in fact an improved version of EPWE [12], similar as IPWE. However, around the locally resonant band gap the conventional EPWE does not match the EPWE. It seems that the EPWE presents a higher ill-conditioned eigenvalue problem than the conventional EPWE around the resonant frequency.

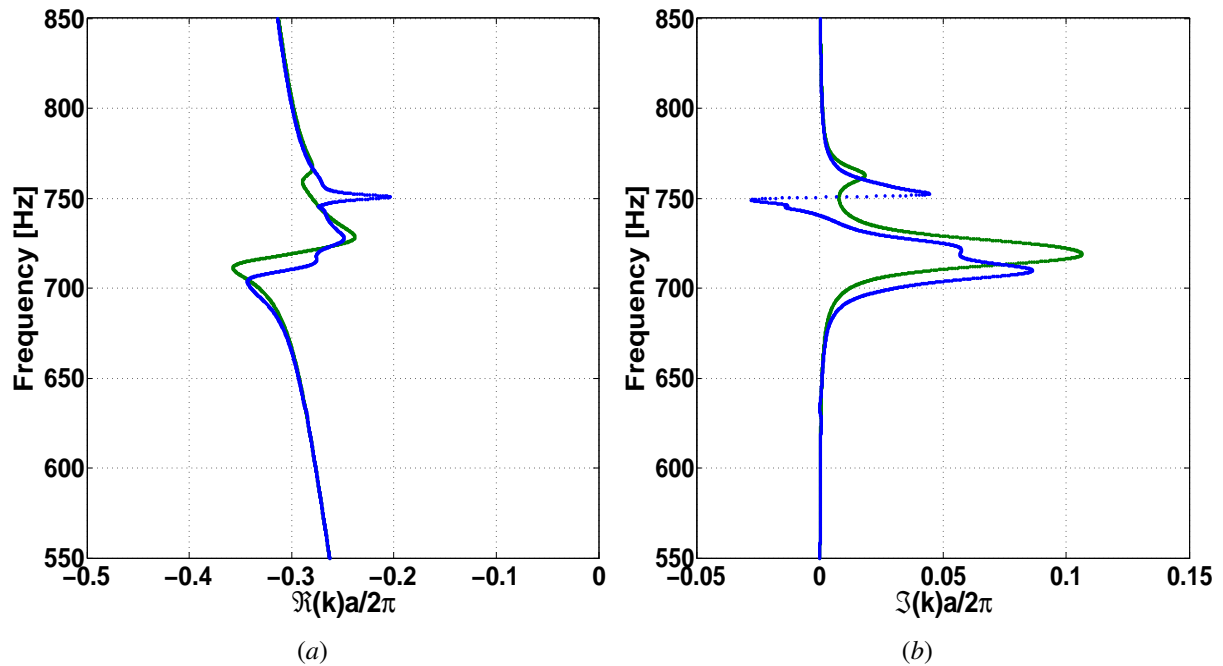


Figure 8. Complex dispersion relation zoom (only the second mode) around the locally resonant band gap of the 2-D PM plate with a resonant circuit ( $f_T = 768.786$  Hz) computed by the EPWE (blue points) and conventional EPWE (green points), considering  $\Delta f = 0.1$  Hz.

### 3 Conclusions

The complex dispersion relations of a 2-D mechanical metamaterial plate with periodic arrays of shunted piezo-patches are investigated. These dispersion relations computed by IPWE and EPWE approaches show good agreement. The Bragg-type band gaps are first observed for the open and short circuits. Next, the resistive and resonant circuits are studied and the locally resonant band gap is opened up for the resonant case. The results can be used for elastic wave attenuation using 2-D piezoelectric periodic structures.

**Acknowledgements.** The authors gratefully acknowledge the support of the Brazilian funding agencies CAPES (Finance Code 001), CNPq (Grant Reference Numbers 313620/2018 and 151311/2020-0), FAPEMA (Grant Reference Numbers 00857/19, 02730/19, 00824/20 and 00133/21) and FAPESP (Grant Reference Number 2018/15894-0).

**Authorship statement.** The authors hereby confirm that they are the sole liable persons responsible for the authorship of this work, and that all material that has been herein included as part of the present paper is either the property (and authorship) of the authors, or has the permission of the owners to be included here.

### References

- [1] S. Chen. Wave propagation in acoustic metamaterials with resonantly shunted cross-shape piezos. *Journal of Intelligent Material Systems*, vol. 29, n. 13, pp. 2744–2753, 2018.
- [2] E. J. P. Miranda Jr., E. D. Nobrega, A. H. R. Ferreira, and J. M. C. Dos Santos. Flexural wave band gaps in a multi-resonator elastic metamaterial plate using Kirchhoff-Love theory. *Mechanical Systems and Signal Processing*, vol. 116, pp. 480–504, 2019.
- [3] E. J. P. Miranda Jr., E. D. Nobrega, S. F. Rodrigues, C. Aranas Jr., and J. M. C. Dos Santos. Wave attenuation in elastic metamaterial thick plates: Analytical, numerical and experimental investigations. *International Journal of Solids and Structures*, vol. 204-205, pp. 138–152, 2020.
- [4] C. Sugino, S. Leadham, M. Ruzzene, and A. Erturk. An investigation of electroelastic bandgap formation in locally resonant piezoelectric metastructures. *Smart Materials and Structures*, vol. 26, n. 055029, 2017.
- [5] A. Aghakhani, M. M. Gozum, and I. Basdogan. Modal analysis of finite-size piezoelectric metamaterial plates. *Journal of Physics D: Applied Physics*, vol. 53, n. 505340, 2020.

- [6] X. Xiao, Z. C. He, E. Li, B. Zhou, and X. K. Li. A lightweight adaptive hybrid laminate metamaterial with higher design freedom for wave attenuation. *Composite Structures*, vol. 243, n. 112230, 2020.
- [7] Y. Cao, Z. Hou, and Y. Liu. Convergence problem of plane-wave expansion method for phononic crystals. *Physics Letters A*, vol. 327, n. 247-253, 2004.
- [8] Y.-C. Hsue, A. J. Freeman, and B.-Y. Gu. Extended plane-wave expansion method in three-dimensional anisotropic photonic crystals. *Physical Review B*, vol. 72, n. 195118, 2018.
- [9] G. Kirchhoff. Über das gleichgewicht und die bewegung einer elastischen scheibe. *Journal für die reine and angewandte Mathematik*, vol. 40, pp. 51–88, 1850.
- [10] A. E. H. Love. The small free vibrations and deformation of a thin elastic shell. *Philosophical Transactions of the Royal Society*, vol. 179, pp. 491–546, 1888.
- [11] L. Brillouin. *Wave propagation in periodic structures*. Dover Publications, New York, 1946.
- [12] E. J. P. Miranda Jr. and J. M. C. Dos Santos. Evanescent Bloch waves and complex band structure in magneto-electroelastic phononic crystals. *Mechanical Systems and Signal Processing*, vol. 112, pp. 280–304, 2018.